

Study on the Adhesion Characteristic between Wheel and Rail using the Scaled Test-bench

Min-Soo Kim

Abstract—Railway vehicles driven by wheels obtain driving force required to propulsion and braking by adhesion force between wheels and rails, this adhesion force is determined by multiplying adhesion coefficient of the friction surface by the applied axle load. In railway system, this adhesion coefficient is usually defined as the maximum traction/braking coefficient. To get the maximum traction/braking force represented as the adhesion coefficient, it is necessary to estimate the adhesion coefficient according to the speed difference between the wheel and the rail on the contact point.

Scaled adhesion test-bench is an experimental device that contacts mutually with disc rollers which are equivalent to wheels and rails of railway vehicles, and rotates mutually by friction by driving each motor connected with roller axes. Test procedure for adhesion characteristics on slip change is following; First, initial speed of the wheel disc with radius 0.1 [m] is set in 1000 [r.p.m] after applying the axle load of wheel/rail as 200 [kgf], then reduce the speed of the rail disc with radius 0.15 [m] from 628 [r.p.m] to 30 [r.p.m] to generate slip while maintaining the initial speed of wheel disc constantly. And test procedure for adhesion comparison under dry and wet is following; First, the wheel disc's (radius 0.15 [m]) initial speed is set in 500 [r.p.m] after applying the axle load of wheel/rail as 142.63 [kgf], then reduce the rail disc's speed from 500 [r.p.m] to 475 [r.p.m] (generates slip) for one minute while maintaining the speed of wheel disc.

This paper also observes the variations in surface roughness and hardness of the wheel/rail discs for the sliding distance in each position and describes the development of a scaled adhesion test-bench for analyzing of the adhesion coefficient between wheel and rail.

Keywords— Test-bench, Adhesion Coefficient, Adhesion Force, Slip, Slide, Axle Load, Railway Vehicle.

I. INTRODUCTION

RAILWAY vehicles driven by wheels obtain force required to propulsion and braking by adhesion force between wheels and rails, this adhesion force is determined by multiplying adhesion coefficient of the friction surface by the applied axle load. That is, adhesion coefficient is determined by environmental conditions (such as temperature, humidity and

This study was financially supported by R&D program “Core Technology(Train Control System, Brake System, Bogie System) Development for Improvement of Railway Vehicle (PK1503F)” of the Korea Railroad Research Institute(KRRI), Republic of Korea.

M. S. Kim is with the Korea Railroad Research Institute, Uiwang-si, Gyeonggi-do, 437-757, KOREA (phone: +82-31-460-5205; fax: +82-31-460-5449; e-mail: ms_kim@krii.re.kr).

surface conditions) and slip velocity (defined as difference between the driving wheel speed and the vehicle speed) [1][2].

According to the slip velocity increase, adhesion coefficient increases to a certain area (the maximum value), it is well known to have a characteristic that after reaching the maximum point it decreases gradually[3][4].

In the operation of railway vehicles, slip and slide (or skid) phenomenon are inevitably occurs. This phenomenon in railway vehicles occurs when the maximum driving force applied between the wheel and rail more than the maximum adhesive force, or when the braking force applied less than the maximum adhesive force. If these slip and slide phenomenon are excessively generated, these cause excessive wear of contact area or it is a factor for reducing tractive force and braking force due to destabilizing control characteristics of driving/braking system. In addition, this phenomenon provides direct causes for vehicle accident, have an important influence upon system safety and economic efficiency. Therefore, many researchers have made great efforts to investigate these effects using the test equipment that can simulate characteristics of slip and skid and have been used to analyze the driving and braking characteristics of railway vehicles and adhesive characteristics in various environments [4]-[6]. In this paper, a scaled adhesion test-bench was developed to analyze adhesive characteristics of wheel and rail, and the adhesion database which is based on rotation with friction was established.

This paper is organized as the followings. Section 2 describes the design of the scaled adhesion test-bench for analyzing the wheel/rail contact. Section 3 deals with experimental results for measurement of adhesion coefficient. The main conclusions are then summarized in section 4.

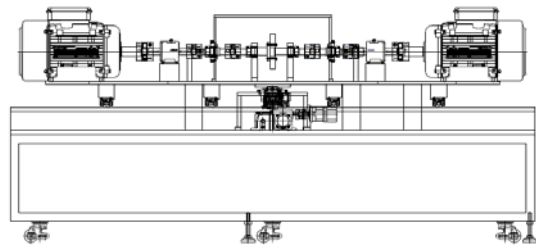
II. DESIGN OF THE SCALED ADHESION TEST-BENCH

A. Design of the Scaled Adhesion Test-bench

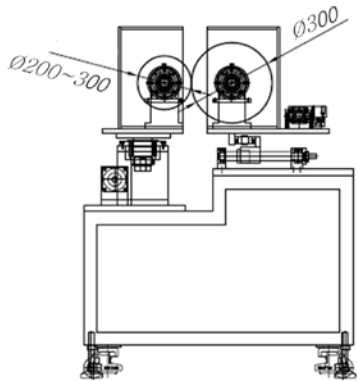
Scaled adhesion test-bench is designed as two disc type to rotate mutually with disc rollers which are equivalent to wheels and rails of railway vehicles, and simulates mutually by friction by driving each motor connected with roller axes.

Therefore, the adhesion test-bench was designed two parts: one is a part of braking motor and the other is a part of driving motor.

Fig. 1 shows the designed adhesion test-bench which is made up of four parts: braking motor parts, driving motor parts, axle load control parts, and angle of attack control parts.



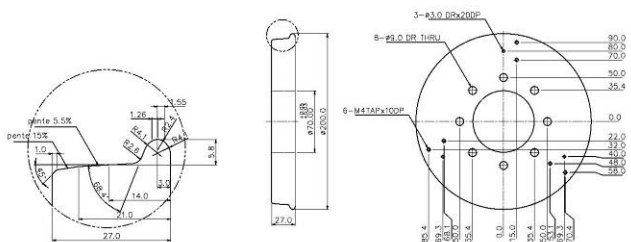
(a) front views of the scaled adhesion test-bench



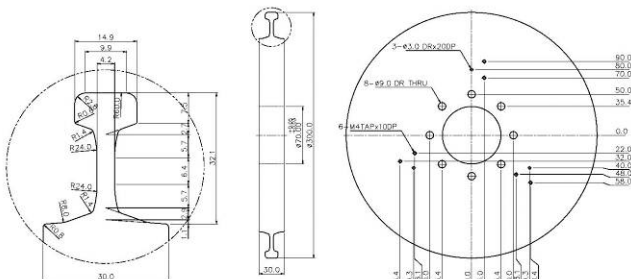
(b) side views of the scaled adhesion test-bench

Fig.1 Drawings of the designed adhesion test-bench

Fig. 2 shows the shape of specimens of the scaled adhesion test-bench representing wheel and rail, and schematic views of two disc adhesion test-bench, respectively.



(a) wheel shape



(b) rail shape

Fig.2 Drawings of specimens

B. Overviews of the Scaled Adhesion Test-bench

Scaled adhesion test-bench is developed for the experimental device to replace the full-scaled system which composites wheel and rail systems of railway vehicles. The scaled adhesion test-bench also was composed of four components which are a part of rail motor, a part of wheel motor, a part of control of the axle load, and a part of control of attack angle, and it designed as the mainly purpose of the research about contact characteristics of wheel/rail and adhesive coefficient.

- A part of rail motor and a part of wheel motor perform the roles that make the rotation speed differences between wheel-rail by rotating disc to simulate the wheel and rail.

- A part of wheel motor consists of a driving motor, a driving motor axis, torque sensor, an encoder and wheel specimens, and a part of rail motor consists of a braking motor, a braking motor axis, torque sensor, an encoder and rail specimens.

- To generate contact force (i.e. axle load) between wheel and rail, a feedback control method which makes movement the entire braking motor axis to another axis in order to simulating the delivered load from wheels to rails is used.

- The part of control of the axle load consists of a stepping motor, ball screw and four LM guides, and it is designed to simulate transmission of the load from wheel to rail in 1.2(kN).

Fig. 3 shows the developed adhesion test-bench for analyzing the adhesion characteristics as a scale model.

A Part of Rail Motor A Part of Wheel Motor



(a) side view of the scaled adhesion test-bench



(b) upper side view of the scaled adhesion test-bench



(c) control console for the scaled adhesion test-bench

Fig.3 Scaled adhesion test-bench for analyzing the adhesion characteristic

Table I describes the main features of the scaled adhesion test-bench.

Table I performance of experimental apparatus

Rotational speed (rpm)	0~1780
Torque (Nm)	0~196.1
Contact load (kgf)	0~500
Attack angle (degree)	-3~3
Slip ratio (%)	0~95

Linear dimension of the rail disc and wheel disc for test specimens are designed to fulfill the 1/5 scale with reference 60 [kg] rail shapes from KSR 9106 standard rail.

III. EXPERIMENTAL RESULTS

A. Adhesion Characteristics Test on Slip Variation

The adhesion test was carried out under the conditions of different wheel/rail contacts, such as various speeds, axle loads, and contamination situation (oil, water, sand, etc.). In order to generate slip, we adapt a method which the rotation speed of the part of the braking motor decrease to zero while maintaining the initial rotation speed of the part of the driving motor constantly to generate speed difference. For example, firstly, the motor of the driving motor axis with a wheel disc rotates 1000(r.p.m), and the motor of the braking motor axis with a rail disc rotates 628(r.p.m). Then, decelerate to the rail disc's speed of rotation to 30(r.p.m) slowly with 200(kgf) of axle load.



Fig.4 specimens of wheel and rail for the scaled adhesion test-bench

In this process, adhesion coefficient was measured by measuring the value of torque sensors that are installed in the axis of the driving motor and the axis of the braking motor.

Slip has a value between 0 and 1, 0 means same rotation rate, and 1 means fully sliding state when one axis of rotation speed becomes zero.

The torque of the wheel is not equal to the torque of the roller. The torque of the driving motor axis M_w is given by (1).

$$M_w = Fr_w \quad (1)$$

where F is the traction force (or adhesion force) and r_w is the radii of the wheel, respectively.

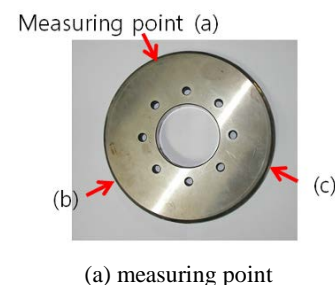
The adhesion coefficient μ is calculated by dividing the tangential force by the normal load as (2)

$$\mu = \frac{F}{N} = \frac{M_w}{Nr_w} \quad (2)$$

where N is axle load.

B. Adhesion Characteristics Test Results on Slip Variation

The variations in surface roughness and hardness of the wheel/rail discs for the sliding distance in each position was observed. The measure points of the wheel specimen and the measuring direction for measuring the surface roughness profiles are shown in Fig. 5.



(a) measuring point



Measuring direction

(b) measuring direction

Fig. 5 measuring point and direction for roughness measurement

The surface roughness profiles and the surface measurement parameters of the rail spacemen at the initial state appear in Fig. 6 and Table II, respectively.



Fig. 6 surface roughness profiles of the rail spacemen at the initial state

Table II initial state of the surface measurement parameters

R_a	R_q	R_z
0.391[μm]	0.507[μm]	2.631[μm]

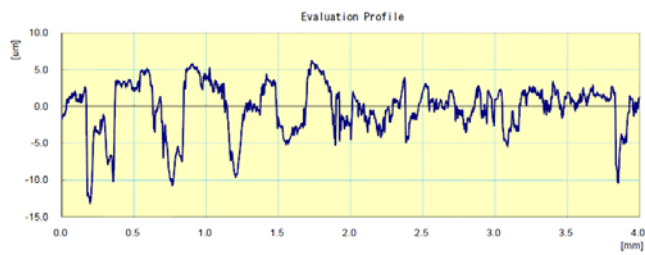
Fig. 7 shows the surface roughness profile in three position of the wheel surface and Table III indicates the surface measurement parameters of the rail spacemen in the same position after the several adhesion tests.



(a) roughness profile of position (a)



(b) roughness profile of position (b)



(c) roughness profile of position (c)

Fig. 7 surface roughness profiles in each position

Table III surface measurement parameters in each position

position	R_a	R_q	R_z
(a)	2.899[μm]	3.746[μm]	16.941[μm]

(b)	2.063[μm]	2.662[μm]	13.241[μm]
(c)	2.633[μm]	3.268[μm]	13.543[μm]

In the table III, R_a is defined as roughness average which is the main height as calculated over the entire measured length or area as (3). And R_q means the root means square (r.m.s) average between the height deviations and the means line/surface taken over the evaluation length/area as (4). Finally, R_z is the average maximum profile of the greatest peak-to-valley separations in the evaluation area. Each parameter is defined as followings.

$$R_a = \frac{1}{n} \sum_{i=1}^n |Y_i - \bar{Y}| \quad (3)$$

$$R_q = \sqrt{\frac{1}{n} \sum_{i=1}^n (Y_i - \bar{Y})^2} \quad (4)$$

Fig. 8 shows the velocity graphs measuring the encoders of the driving/braking motor axis, the rail-axis torque graph, and the wheel-axis torque graph, collecting the torque sensors installed between motor and the wheel/rail specimens.

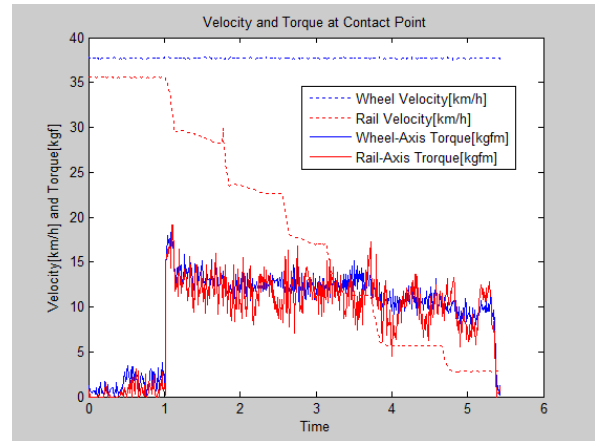


Fig. 8 velocity graphs and torque graphs

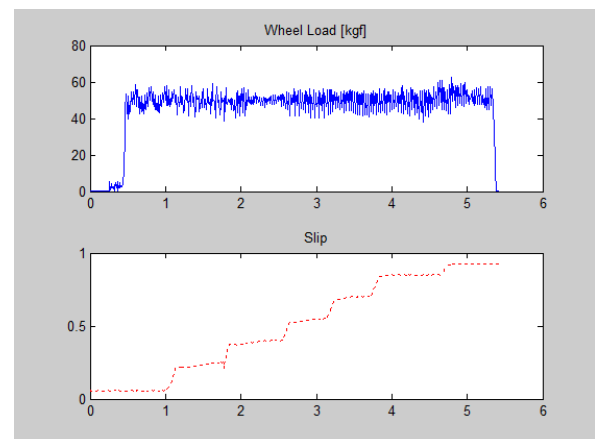


Fig. 9 normal loads and slip ratio graphs

Fig. 9 shows the normal load and slip ratio which is defined as a difference velocity.

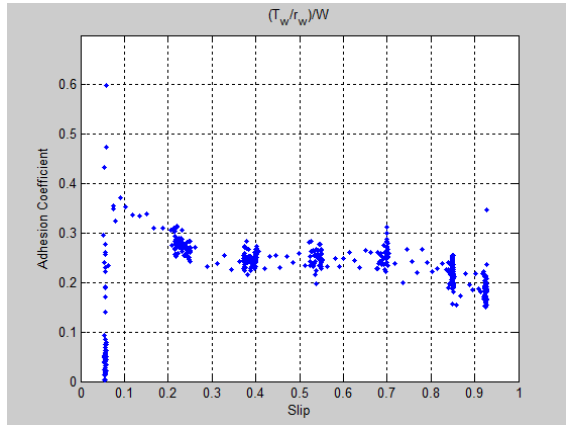


Fig. 10 adhesion coefficient after converting processing

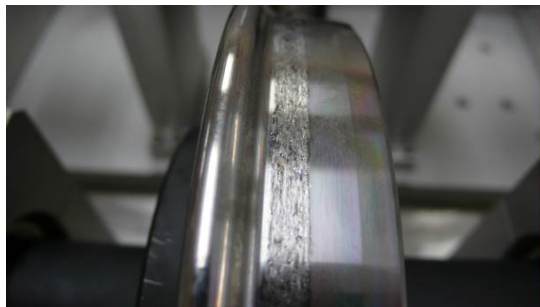
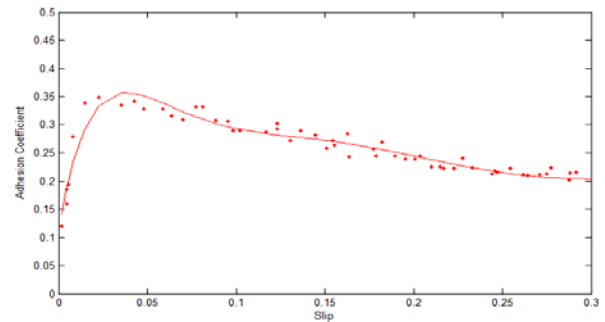
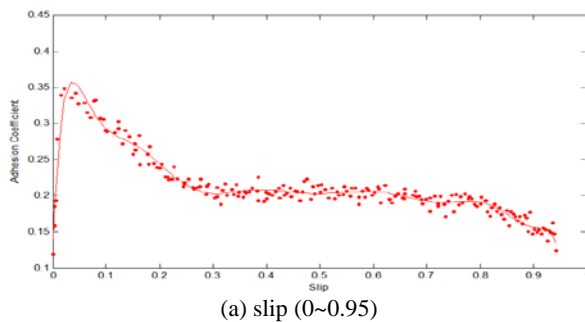


Fig. 11 surface of the test wheel

The torque values of the driving/braking motor axis and axle load for calculating the adhesion coefficient were collected and rearranged according to variation of the slip from 0 to 1.

Fig. 12-(a) illustrates the calculated slip ratio by converting linear velocity vs. adhesion coefficient based on torque sensor values and normal load values at the each contact points. When the slip varies from 0 to 0.95 the characteristic of the adhesion coefficient and its enlarged results from 0 to 0.3 are shown in Fig. 12-(b).



(b) slip (0~0.3)

Fig.12 adhesion coefficient when the axle load 200 (kgf) is applied

C. Adhesion Test between Dry and Wet Condition

In this experiment, adhesion test between dry and wet condition were performed to compare the differences between those conditions. The test procedure is following; First, initial speed of the wheel disc with radius 0.15[m] is set in 500[r.p.m] applying the axle load of wheel/rail as 142.63[kgf], then reduce the speed of the rail disc with radius 0.15[m] from 500[r.p.m] to 475 [r.p.m] for 30 seconds (i.e. generates slip) while maintaining the initial speed of wheel disc.

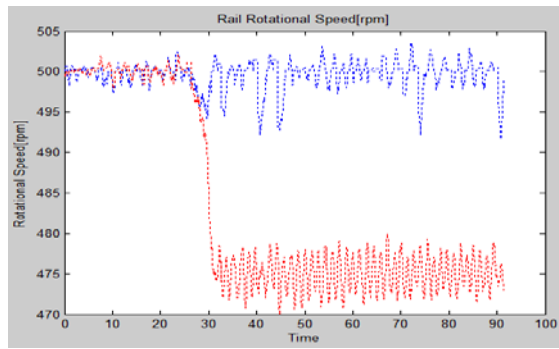


Fig.13 Experimental environments: wheel and rail speed, torque, and axle load

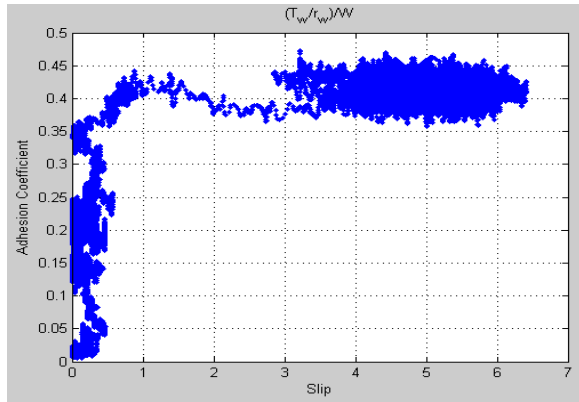
Fig.13 shows the velocity graphs measuring the encoders of the driving and braking motor axis, and rail the torque graphs collecting the torque sensors installed between motor and the wheel/rail specimens.

D. Adhesion Test Results between Dry and Wet Condition

Fig. 14-(a) and 15-(a) illustrate the rotational speed of wheel disc and rail disc, and Fig. 14-(b) and 15-(b) represents the calculated slip ratio by converting linear velocity vs. adhesion coefficient based on torque sensor values at the contact point in each dry and wet conditions. When the slip varies from 0[%] to 5[%], the characteristic of the adhesion coefficient are well expressed in Fig.14-(b) and 15-(b), respectively.



(a) rotational speed of wheel disc and rail disc



(b) adhesion coefficient

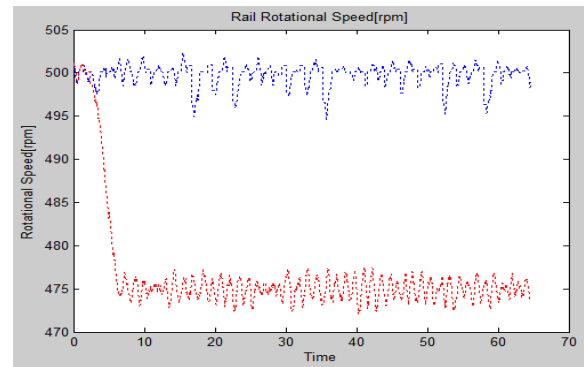
Fig.14 experimental results: rotational speed differences and adhesion coefficient in dry condition

Table IV indicates the data comparison of the experimental results after the several adhesion tests (dry and wet condition).

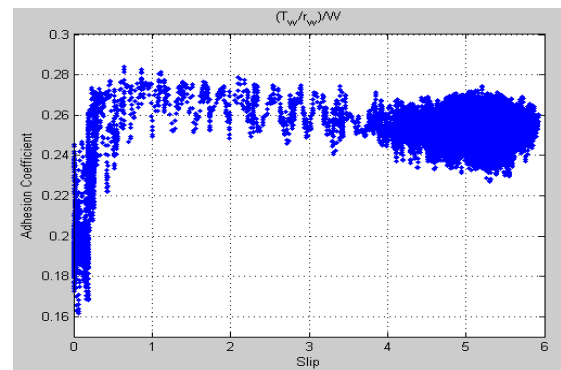
Table IV Data comparison of experimental results (dry and wet condition)

Condition	Properties	1st	2nd
Dry	Mean values of wheel load [kgf]	137.867	137.855
	Mean values of slip ratio [%]	5.116	5.097
	Mean values of adhesion coefficient	0.412	0.417
	Mean values of adhesion coefficient (remove the bios)	0.22	0.23
Wet	Mean values of wheel load [kgf]	137.317	137.12
	Mean values of slip ratio [%]	5.089	5.109
	Mean values of adhesion coefficient	0.255	0.221

Mean values of adhesion coefficient (remove the bios)	0.07	0.08
---	-------------	-------------



(a) rotational speed of wheel disc and rail disc



(b) Adhesion coefficient

Fig.15 experimental results: rotational speed differences and adhesion coefficient in the wet condition

As the adhesion coefficient was measured relatively high at two conditions, we guessed that the torque value caused from the load value between wheels and rails was not removed. Therefore, we try to eliminate the effect of the bios value as the initial contact load between wheels and rails. As we compared the adhesion coefficient, the friction coefficient in dry condition was calculated one and half times higher than in wet. It had similar characteristics with the adhesion coefficient calculated in an actual experiment, which was 0.25~0.30 in dry and 0.18~0.2 in wet.

IV. CONCLUSION

In this paper, a scaled adhesion test-bench is utilized to analyze the adhesion characteristics of wheels and rail, which are designed the twin disc type.

Firstly, adhesion trend test on the slip variation was carried out. That is, adhesion test procedure for fluctuations of the adhesion coefficient according to the slip variation is following; First, the wheel disc's (radius 0.1[m]) initial speed is set in 1000 [r.p.m] after applying the axle load of wheel/rail as 200[kgf], then reduce the rail disc's speed from 628[r.p.m] to 30[r.p.m] to generate slip while maintaining the speed of wheel disc

constantly. The test result clearly shows that the maximum adhesion coefficient is calculated at the slip value 0.05 when the slip varies from 0 to 0.95.

Secondly, adhesion test between dry and wet condition were performed to compare the differences between two conditions. Test procedure for adhesion comparison under dry and wet is following; First, the wheel disc's (radius 0.15[m]) initial speed is set in 500[r.p.m] after applying the axle load of wheel/rail as 142.63[kgf], then reduce the rail disc's speed from 500[r.p.m] to 475[r.p.m] (generates slip) for one minute while maintaining the speed of wheel disc. After generating the slip velocity between wheels and rails, we collected data maintaining a slip state for 1 minute right after stabilizing the torque value. It was found from the experiment results that it had similar characteristics with the adhesion coefficient calculated in an actual experiment, which was 0.25~0.30 in dry and 0.18~0.2 in wet.

REFERENCES

- [1] Simon Iwnicki, *Handbook of Railway Vehicle Dynamics (Eds)*, Taylor&Francis, 2006.
- [2] H. Harrison, T. McCanney, and J. Cotter, "Recent developments in coefficient of friction measurements at the rail/wheel interface," *Wear* 253, pp. 114 ~ 123, 2002.
- [3] H. Chena, M. Ishida, A. Namuraa, K-S Baekb, T. Nakaharac, B. Leband, M. Paud., "Estimation of wheel/rail adhesion coefficient under wet condition with measured boundary friction coefficient and real contact area," *Wear* 271, Issues 1-2, pp. 32 ~ 39, 2011.
- [4] Weihua Xhang, Jianzheng Chen, Xuejie Wu, and Xuesong Jin, "Wheel/rail adhesion and analysis by using full scale roller rig," *Wear* 253, pp. 82 ~ 88, 2002.
- [5] H. Chen, T. Ban, M. Ishida, M. Ishida, and T. Nakabara, "Adhesion between rail/wheel under water lubricated contact," *Wear* 253, pp.75 ~ 81, 2002.
- [6] Kiyoshi Ohishi, Yasuaki Ogawa, "Adhesion Control for Electric Motor Coach Based on Force Control Using Disturbance Observer," *AMC2000- NAGOYA*, pp.323-328, 2000.
- [7] Yosuke Takaoka, Atsuo Kawamura, "Disturbance Observer Based Adhesion Control for Sinkansen," *AMC2000- NAGOYA*, pp.169-174, 2000.
- [8] Atsuo Kawamura, Keiichi Takeuchi, Takemasa Furuya, "Measurement of the Tractive Force and the New Adhesion Control by the Newly Developed Tractive Force Measurement Equipment," *PCC-Osaka*, pp.879-884, 2000.
- [9] S. Kumar, M. F. Alzoubi, and N. A. Allsayyed, "Wheel/rail adhesion wear investigation using a quarter scale laboratory testing facility," *Proceedings of the 1996 ASME/IEEE Joint Railroad Conference*, 1996
- [10] S. Kadowaki, K. Ohishi, Yasukawa and T.Sano, "Anti-skid re-adhesion control based on disturbance observer considering air brake for electric commuter train," *Proc. 8th IEEE Int. Workshop Advanced Motion Control*, Kawasaki, Japan, pp.607-612, 2004
- [11] S. Shirai, "Adhesion Phenomena at high-speed range and performance of an improved slip-detector," *Q.Rep. Railw. Tech Res. Inst.*, vol. 18, no. 4, pp.189-190, 1977
- [12] I. P. Isaev and A. L. Golubenko, "Improving experimental research into adhesion of the locomotive wheel with the rail," *Rail Int.*, vol. 20, no8, pp.3-10,1989
- [13] T.Ohyama, "Some basic studies on the influence of surfaced contamination on adhesion force between wheel and rail at high speed," *Q.Rep.Railw.Tech.Res.Inst.*, vol.30, no. 3, pp.127-135,1989
- [14] K.Ohishi, K. Nakano, I.Miyashita, and S.Yasukawa, "Anti-slip control of electric motor coach based on disturbance observer." *Proc. 5th IEEE Int. Workshop Advanced Motion Control*, Coimbra Portugal, pp.580-585,1998
- [15] T.Watanabe and M.Yamashita, "A novel anti-slip control without speed sensor electric railway vehicles," *Proc.27th Annu. Conf.IEEE Industrial Electronics Society*, Denver, CO, vol.2, pp.1382-1387,2001
- [16] M.C. Wu and M.C.Shih, "Simulated and experimental study of hydraulic anti-lock braking system using sliding-mode PWM control," *Mechatronics*, vol.13, pp.331-351, 2003
- [17] A.Kawamura, T.Furuta, K.Takeuchi, Y.Takaoka, Y.yoshimoto, and M.Aco, "Maximum adhesion control for Shinkansen using the tractive force tester," *proc. IEEE Power Conversion Conf.*, Osaka, Japan, vol.1, pp.567-572, 2002
- [18] Y.Ishikawa and A.Kawamura, "Maximum adhesion force control in super high speed train," *Proc. IEEE Power Conversion Conf.*, Nagaoka, Japan, vol.2, pp.951-954,1997
- [19] Y.Takaoka and A.Kawamura, "Disturbance observer based adhesion control for Shinkansen," *Proc. IEEE Int. Workshop Advanced Motion Control*, Nagoya, Japan, pp.169-174, 2000
- [20] C.Canudas de Wit, K.J. Astrom, and P.Lischinsky, "A new model for control of systems with friction," *IEEE Trans. Automat. Contr.*, wol.40, no.3, pp.419-425, 1995.
- [21] T.A.Johansen, I.Petersen, J.Kalkkuhl, and J.Luschinsky, "Gain-scheduled wheel slip control in automotive brake system," *IEEE Trans. Contr. Syst.Technol.*, vol.11 no.6,pp.799-811, 2000.
- [22] L.Alvarez, J.Yi, R.Horowitz, and L.Olmos, "Dynamic friction model-based tire-road friction estimation and emergency braking control," *ASME J.DYN. Syst., Meas. Contr.*, vol.127, no.1, pp.22-32, 2005
- [23] J.Yi, L.Alvarez, and R.Horowitz, "adaptive emergency braking control with underestimation of friction coefficient." *IEEE Trans. Contr. Syst. Technol.*, vol.10, no.3, pp.381-392, 2002.
- [24] F.Gustafsson, "Slip-based tire-road friction estimation," *Automatica*, vol.33, no.6, pp.1087-1099, 1997.
- [25] S. Kumar, M.F. Alzoubi, and N.A. Allsayyed. "Wheel/rail adhesion wear investigation using a quarter scale laboratory testing facility," *Proc. 1996 ASME/IEEE Joint Railroad Conf.*, Oakbrook, IL, pp. 247-254, 1996
- [26] X.S. Jin, W.H. Zhang, J. Zeng, Z.R. Zhou, Q.Y. Liu, and Z.F. Wen, "Adhesion experiment on a wheel/rail system and its numerical analysis," *IMEchE J. Eng. Tribology*, vol. 218, pp. 293-303, 2004.
- [27] W.Zhang, J.Chen, X.Wu, and X.Jin, "Wheel/rail adhesion and analysis by using full scale roller rig," *Wear*, vol. 253, no.1, pp.82-88, 2004.
- [28] H. Sakai, *Tire Engineering*, Tokyo, Japan: Grand Prix Pub-lishing, 1987
- [29] J.J. Kalker and J. Piotrowski, "Some new results in rolling contact," *Veh. Syst. Dyn.*, vol. 18, no.4, pp.223-242, 1989.
- [30] J.J. Kalker, *Three-Dimensional Elastic Bodies in Rolling Contact*. Norwell, MA:Kluwer Academic, 1990.
- [31] K. Knothe and S. Liebelt, "Determination of temperatures for sliding contact with applications for wheel-rail systems," *Wear*, vol. 189,pp. 91-99, 1995.
- [32] P. Dahl, Solid friction damping of mechanical vibrations," *AIAA J.*, vol. 14, no. 12, pp. 1675-1682, 1976.
- [33] C. Canudas de Wit and P. Tsiotras, "Dynamic tire friction models for vehicle traction control," *Proc. 38th IEEE Conf. Decision Control*, Phoenix, AZ, pp. 3746-3751, 1999
- [34] C. Canudas de Wit and P. Lischinsky, "Adaptive friction compensation with partially known dynamic model," *Int. J. Adapt. Contr. Signal Process.*, vol. 11, pp. 65-80, 1997.
- [35] G. Charles and R. Goodall, "Low adhesion estimation", *Proc. Institution Engineering Technology Int. Conf. Railway Condition Monitoring*, Birmingham., UK, pp. 96-101, 2006
- [36] Y. Shimizu, K. Ohishi, T. Sano, S. Yasukawa, and T. Koseki, Anti-slip/skid readhesion control based on disturbance observer considering bogie vibration, *Proc. 4th Power Conversion Conf.*, Nagoya, Japan, pp. 1376-1381, 2007
- [38] S. Uchida, Brake of railway III, *Japan Train Oper. Assoc. J. Brake of Rail-way Vehicles*, vol. 3, pp. 25-28, 2001.
- [39] W. Gao and J.C. Hung, "Variable structure control of nonlinear systems," *IEEE Trans. Ind. Electron.*, vol. 40, no. 1, pp. 45-55, 1993.
- [40] K.J. Lee, H.M. Kim, and J.S. Kim, "Design of a chattering-free sliding mode controller with a friction compensator for motion control of a

- ball-screw system,” *IMEchE J. Syst. Contr. Eng.*, vol. 218, pp. 369-380, 2004.
- [41] H. K. Khalil, *Nonlinear Systems*. Englewood Cliffs, NJ: Prentice-Hall, 1996.
- [42] M. S. Kim, Y. S. Byun, Y. H. Lee and K. S. Lee, “Gain Scheduling Control of Levitation System in Electromagnetic Suspension Vehicle,” *WSEAS Transactions on Circuits and Systems*, Vol.5, pp.1706-1712, 2006.
- [43] M. S. Kim, Y. S. Byun and H. M. Hur, “Design of the Active Steering Controller of Scaled Railway Vehicle Improving Curving Performance,” *The 7th WSEAS Int. Conf. on Circuits Systems, Electrics, Control & Signal Processing*, 2008
- [44] M. S. Kim, J. H. Park, and W. H. You, “Construction of Active Steering Control System for the Curving Performance Analysis of the Scaled Railway Vehicle,” *The 7th WSEAS Int. Conf. on Circuits Systems, Electrics, Control & Signal Processing*, 2008
- [45] M-S Kim, Y-S Byun, H-M Hur, “Design of Active Steering Controller of the Scaled Railway Vehicle,” *International Journal of Circuits, Systems and Signal Processing*, Vol.2 No.3, 2008.
- [46] M-S Kim, J-H Park, W-H You, “Construction of Active Steering System of the Scaled Railway Vehicle,” *International Journal of Systems Applications, Engineering & Development*, Vol.2, No.4, 2008.
- [47] M-S Kim, “Design of the Active Steering Fuzzy Controller with the Degree of Non-uniformity for a Scaled Railway Vehicle,” *The 9th WSEAS International Conference on Robotics, Control and Manufacturing Technology (ROCOM '09)*, Hangzhou, China, May 20-22, 2009.
- [48] M-S Kim, H-M Hur, J-H Park and W-H You, “Performance Measurement Systems of the Scaled Active Steering Railway Vehicle using the Telemetry Systems,” *The 10th WSEAS International Conference on Signal Processing, Computational Geometry and Artificial Vision*, Taipei, Taiwan, August 20-22, 2010.
- [49] M-S Kim, H-M Hur, “Detection of the Wheel-rail Lateral Displacement based on the Image Processing Method,” *The 13th Asia-Pacific Conference on Non-Destructive Testing*, 2009.
- [50] M-S Kim, H-M Hur, J-H Park and W-H You, “Remote Sensing of the Lateral Force for the Scaled Active Steering Railway Vehicle,” *International Journal of Systems Applications, Engineering & Development*, Issue 1, Volume 5, 2011.
- [51] M-S Kim, “Measurement of the Wheel-rail Relative Displacement for the Active Wheelsets Steering System using the Image Processing Algorithm,” *The 4th WSEAS International Conference on Visualization, Imaging and Simulation*, Catania, Italy, November 3-5, 2011.
- [52] M-S Kim, “Measurement of the Wheel-rail Relative Displacement using the Image Processing Algorithm for the Active Steering Wheelsets,” *International Journal of Systems Applications, Engineering & Development*, Issue 1, Volume 6, 2012.
- [53] M-S Kim and N-P Kim, “Design of the Scaled Adhesion Tester for Analyzing the Adhesion Characteristic of Railway Vehicles,” *The 8th WSEAS International Conference on REMOTE SENSING (REMOTE '12)*, Prague, Czech Republic, September 24-26, 2012.
- [54] M-S Kim, “Analysis of the Wheel/rail Adhesion Characteristic using the Scaled Adhesion Tester,” *5th European Conference of MECHANICAL ENGINEERING (ECME '14)*, Florence, Italy November 22-24, 2014.

Min-Soo Kim received the B.S., M.S., and Ph.D. degrees in electrical engineering from Soongsil University, Seoul, Korea in 1995, 1997, and 2003, respectively. From December 2005 he is a senior researcher at the Metropolitan Transit System Research Division, Metropolitan Transportation Research Center, at Korea Railroad Research Institute, 360-1 Woram-dong, Uiwang-si, Kyonggi-do, 437-757 Korea (corresponding author to provide phone: +82-31-460-5205; fax: +82-31-460-5449; e-mail: ms_kim@krri.re.kr). His research interests include control systems design of railway vehicle and dynamometer test for the railway brake components.